

# Passivity-Based Iterative Learning Control for Cycling Induced by Functional Electrical Stimulation With Electric Motor Assistance

Vahideh Ghanbari<sup>1b</sup>, Victor H. Duenas<sup>2b</sup>, Panos J. Antsaklis<sup>1b</sup>, and Warren E. Dixon<sup>1b</sup>

**Abstract**—This brief examines the use of a learning control method in a passivity-based framework to control a motorized cycle-rider system with functional electrical stimulation (FES) of the quadriceps muscle groups. FES cycling with motorized assistance has been used in the rehabilitation of people with neurological conditions. The concepts of adaptation and passivity are explored to compensate for the uncertain nonlinear time-varying dynamics of the motorized FES cycle-rider system. The system is modeled as a closed-loop feedback, state-dependent switched system such that in each cycle, the quadriceps muscle groups produce the functional torque and the electric motor provides assistance as needed. The output strictly passive feature of the closed-loop system is proven by considering a learning control input. Then, an adaptive update law, based on iterative learning control, is developed to guarantee the convergence of the cadence tracking error. Experimental results from seven able-bodied participants are presented and discussed to demonstrate the effectiveness of this approach. The average cadence tracking error is  $0.00 \pm 2.47$  rpm for the desired trajectory of 50 rpm.

**Index Terms**—FES cycling, functional electrical stimulation (FES), iterative learning control (ILC), medical robotics, nonlinear systems, passivity, switching control, time-varying systems.

## I. INTRODUCTION

**F**UNCTIONAL electrical stimulation (FES) utilized in the lower body is a well-known rehabilitation technique, where muscle contractions are triggered due to the potential field applied across muscle groups to evoke functional tasks [1]. Specifically, FES cycling is applied to people with neurological disorders such as spinal cord injury, stroke, or traumatic brain injury. FES has several therapeutic benefits resulting in the improvement of muscle strength [2]. The FES cycle-rider dynamic model is a complex nonlinear system due to the time-varying nature of the muscle dynamics, the presence of disturbances, input delay, and muscle fatigue. Various control methods have been designed for FES applications such as proportional-derivative and proportional-integral-derivative controllers [3], [4], or optimal control schemes [5].

Manuscript received May 5, 2017; revised January 17, 2018 and May 22, 2018; accepted June 27, 2018. Date of publication July 31, 2018; date of current version August 6, 2019. Manuscript received in final form July 6, 2018. This work was supported in part by NSF under Project 1762829 and in part by AFOSR under Grant FA9550-18-1-0109. Any opinions, findings and conclusions or recommendations expressed in this material are those of the authors and do not necessarily reflect the views of the sponsoring agency. Recommended by Associate Editor A. Serrani. (*Corresponding author: Vahideh Ghanbari.*)

V. Ghanbari and P. J. Antsaklis are with the Department of Electrical Engineering, University of Notre Dame, Notre Dame, IN 46556 USA (e-mail: vghanbar@nd.edu; pantsakl@nd.edu).

V. H. Duenas and W. E. Dixon are with the Department of Mechanical and Aerospace Engineering, University of Florida, Gainesville, FL 32611-6250 USA (e-mail: vhduenas@ufl.edu; wdixon@ufl.edu).

Color versions of one or more of the figures in this paper are available online at <http://ieeexplore.ieee.org>.

Digital Object Identifier 10.1109/TCST.2018.2854773

During FES cycling, muscle forces produce torque primarily about the knee joint, which is transferred to torque about the crank axis. However, there are regions of the crank cycle, where torque production is kinematically inefficient, and thus for efficient cycling the FES contribution is restricted to certain regions of the crank cycle. To maintain a constant cadence, an electric motor is used in the regions where it is inefficient to stimulate the muscle groups. The combination of FES and motor assist makes the overall system a state-dependent switched system. In [6], switching between the muscle stimulation and a motor assist is studied to address the muscle fatigue. Motorized FES cycling systems are studied in [7] to track a desired cadence and power output simultaneously. Since the automatic cycle-rider process is repetitive and possesses a number of uncertainties in its dynamics, the utilization of a learning control technique such as iterative learning control (ILC) scheme is very desirable.

ILC is a well-established adaptive technique for repetitive tasks in which the control input is updated in each trial, based on the previous performance information [8]. For cyclic or repetitive nonlinear time-varying systems, ILC represents a promising learning control method to achieve the asymptotic tracking. This brief employs ILC since the dynamics of the motorized FES cycle-rider system are repetitive. The purpose of ILC is to obtain the asymptotic tracking and to improve the performance of such system after a certain number of cycles/iterations. In [9] and [10], ILC is applied for the robust tracking control of FES systems, and FES-induced cycling based on the repetitive learning control is studied in [11]. FES of the upper limbs using ILC for rehabilitation purposes is studied in [12]. In [13], a fully saturated learning law and an iterative learning formulation are designed to prove the convergence of the states to zero. A nonlinear discrete model is decomposed into linear time-varying systems that can be solved using a global convergent iterative method, such as Newton's method in [14]. The Newton-based ILC method [14] requires the model to be linearized and the initial condition of the control input to be close to the desired state. The dynamic model of the cycle-rider system has uncertainties, nonlinearities, and unknown parameters. Thus, the strategy in this brief is to use a more general form of the ILC control (as a feedforward controller) in conjunction with a robust controller to achieve the convergence to zero of the cadence tracking error. The use of an integral of a kernel multiplied by an influence function is used in [15] to estimate a nonlinear disturbance function that can be repetitive; the resulting learning algorithm ensures asymptotic convergence. However, in comparison with such previous Lyapunov-based methods, the current paper uses a combination of adaptation

and passivity to show  $\mathcal{L}_2$  convergence of the closed-loop system's output.

Passive systems are the most known classes of dissipative systems. In passivity, the energy that is supplied into the system must be greater than or equal to the energy being stored by the system (the storage function), over a certain time interval [16]. The rest of the energy is dissipated. The fundamental concepts of stability and passivity are based on the proper choice of a positive definite function. In Lyapunov theory, this function is known as the Lyapunov function and is used in the stability analysis [17]. In passivity-based approaches, this function is referred to as the storage function. In [18], the passivity is used to demonstrate the global asymptotic stability of several adaptive and learning controllers for robot manipulators including the repetitive learning algorithm developed in [15]. Moreover, a passivity-based iterative learning is used in [19] to learn a desired motion and to achieve the impedance matching by using a saturated position tracking error. In [20] and [21], the passivity-based control and ILC were utilized for robot manipulators with antagonistic biarticular muscles. However, unlike in [21], this brief studies the passivity and adaptation of the nonlinear cycle-rider system with FES applied to lower limb muscles along with the motorized assistance. The closed loop-system is viewed as a switched system, since it switches between muscle groups and the motor assist in each cycle. The learning control method, which is built upon the passivity concept, is employed to cope with system's repetitive nature and to guarantee the convergence of the output error trajectory to zero. To the best of our knowledge, this is the first time that the concept of the passivity and learnability are applied to the motorized nonlinear cycle-rider system with switched control inputs.

This brief is organized as follows: in Section II, preliminaries and background mathematics are introduced. In Section III, the main results are presented, followed by experimental results in Section IV, and in Section V concluding remarks are discussed.

## II. BACKGROUND AND PRELIMINARIES

### A. Dynamic Model

The rider's passive limb dynamics are modeled as a single-degree-of-freedom system [22] as

$$M(q(t))\ddot{q}(t) + V(q(t), \dot{q}(t))\dot{q}(t) + b_{\text{cycle}}\dot{q}(t) + G(q(t)) + P(q(t), \dot{q}(t)) + d_r(t) = \tau_a + \tau_{\text{motor}} \quad (1)$$

where  $q : \mathbb{R}_{\geq 0} \rightarrow \mathcal{Q}$  ( $\mathcal{Q} \subset \mathbb{R}$  denotes the set of crank angles) is the crank angle,  $\dot{q}, \ddot{q} : \mathbb{R}_{\geq 0} \rightarrow \mathbb{R}$  are the velocity and acceleration, respectively,  $M : \mathcal{Q} \rightarrow \mathbb{R}_{>0}$  is the unknown rider and cycle inertia,  $V : \mathcal{Q} \times \mathbb{R} \rightarrow \mathbb{R}$  denotes the centripetal and Coriolis forces,  $b_{\text{cycle}} \in \mathbb{R}_{>0}$  is the damping in the cycle,  $G : \mathcal{Q} \rightarrow \mathbb{R}$  represents the gravitational effects, and  $P : \mathcal{Q} \times \mathbb{R} \rightarrow \mathbb{R}$  accounts for the passive viscoelastic tissue forces in the knee joints. Also, the effects of unknown disturbances from the rider and cycle such as load changes are denoted by  $d_r(t) : \mathbb{R}_{\geq 0} \rightarrow \mathbb{R}$ . The disturbance is assumed to have a known bound as  $|d_r(t)| \leq c_{d_r}$ , where  $c_{d_r} \in \mathbb{R}_{>0}$  is a known constant. In (1),  $\tau_a : \mathcal{Q} \times \mathbb{R} \times \mathbb{R}_{\geq 0} \rightarrow \mathbb{R}$  is the net torque

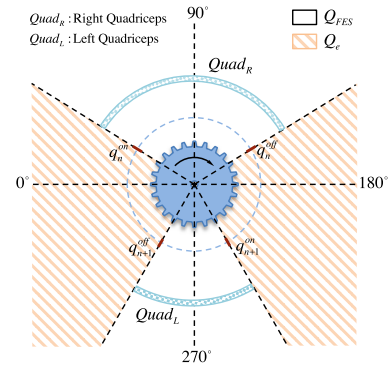


Fig. 1. Switched system pattern shows the range of one cycle, in which the quadriceps muscle groups are stimulated ( $Q_{\text{FES}}$ ), and the range where the electric motor generates the motion ( $Q_e$ ).

produced by active contractions of the rider's muscles and it is defined as

$$\tau_a \triangleq \sum_{m \in \mathbb{M}} B_m(q(t), \dot{q}(t))u_m(t) \quad (2)$$

where  $B_m : \mathcal{Q} \times \mathbb{R} \rightarrow \mathbb{R}$  is the uncertain control effectiveness of a muscle group with subscript  $m \in \mathbb{M} \triangleq \{\text{set of active muscles from right and left legs}\}$  and  $u_m : \mathbb{R}_{\geq 0} \rightarrow \mathbb{R}$  is the electrical stimulation intensity applied to each muscle group. In addition,  $\tau_{\text{motor}} : \mathbb{R}_{\geq 0} \rightarrow \mathbb{R}$  is the torque about the crank axis provided by an electric motor. The torque applied by the motor is

$$\tau_{\text{motor}}(t) \triangleq B_e u_e(t) \quad (3)$$

where  $B_e \in \mathbb{R}$  is a constant relating the current in the electric motor to the resulting torque about the crank axis and  $u_e : \mathbb{R}_{\geq 0} \rightarrow \mathbb{R}$  is the current applied to the motor.

### B. Switched System Model

This brief uses a motorized cycle combined with FES. Lower limb muscles are stimulated to generate the forward pedaling, and an electric motor assists on the regions where FES-induced torque is absent. The system is an arbitrary, state-dependent switched system since the system switches between two modes, the FES mode and the motor mode in each cycle [23]. In other words, the muscle stimulation and the motor assist contribution are limited to certain portions of each cycle (Fig. 1). The electric motor region denoted by  $Q_e \subset \mathcal{Q}$  (where the electric motor is active) and the stimulation region denoted by  $Q_m \subset \mathcal{Q}$  for  $m \in \mathbb{M}$  (where the muscle groups are stimulated).

The union of the stimulation regions is defined as  $Q_{\text{FES}} \triangleq \bigcup_{m \in \mathbb{M}} Q_m$ . Therefore, the region where the electric motor is active is defined as  $Q_e \triangleq \mathcal{Q} \setminus Q_{\text{FES}}$ . Fig. 1 depicts how the switching occurs among different modes (the FES region and the electric motor region) for one cycle. The known sequences of switching states are denoted by  $\{q_0^{\text{on}}, q_0^{\text{off}} \in \mathcal{Q}\}_{n=0}^{\infty}$ , and the corresponding unknown switching times are denoted by  $\{t_0^{\text{on}}, t_0^{\text{off}} \in \mathbb{R}_{\geq 0}\}_{n=0}^{\infty}$ , where each on-time  $t_0^{\text{on}}$  and off-time  $t_0^{\text{off}}$  denotes the instant when  $q$  reaches the corresponding on-angle

$q_0^{\text{on}}$  and off-angle  $q_0^{\text{off}}$ , respectively [24]. The switching laws can be defined for each muscle group,  $\sigma_m : \mathbb{Q} \rightarrow \{0, 1\}$ , and for the electric motor,  $\sigma_e : \mathbb{Q} \rightarrow \{0, 1\}$  as

$$\sigma_m \triangleq \begin{cases} 1 & \text{if } q(t) \in \mathcal{Q}_m \\ 0 & \text{if } q(t) \notin \mathcal{Q}_m \end{cases} \quad \sigma_e \triangleq \begin{cases} 1 & \text{if } q(t) \in \mathcal{Q}_e \\ 0 & \text{if } q(t) \notin \mathcal{Q}_e. \end{cases} \quad (4)$$

The muscle stimulation input,  $u_m$ , and the motor input,  $u_e$ , are defined as in [24] and [25]

$$\begin{aligned} u_m(t) &= k_m \sigma_m(q(t)) u_{\text{FES}}(t) \\ u_e(t) &= k_e \sigma_e(q(t)) u_{\text{motor}}(t) \end{aligned} \quad (5)$$

where  $k_m, k_e \in \mathbb{R}_{>0}$  are the positive constant gains, and

$$u(t) \triangleq u_{\text{FES}} = u_{\text{motor}}. \quad (6)$$

Therefore, the nonlinear dynamics of motorized cycle-rider system with electrical stimulation can be modeled as [25]

$$\begin{aligned} M(q(t))\ddot{q}(t) + V(q(t), \dot{q}(t))\dot{q}(t) + b_{\text{cycle}}\dot{q}(t) + G(q(t)) \\ + P(q(t), \dot{q}(t)) + d_r(t) = B_\sigma(q(t), \dot{q}(t))u(t) \end{aligned} \quad (7)$$

where

$$B_\sigma \triangleq \sum_{m \in \mathbb{M}} B_m k_m \sigma_m + B_e k_e \sigma_e \quad (8)$$

and  $B_\sigma \in \mathbb{R}_{>0}$  is the switched control effectiveness that accounts for the combination of the control effectiveness of each muscle group and the electric motor.

The switched system represented by (7), has the following properties.

*Property 1:*  $\underline{M} \leq M \leq \bar{M}$ , where  $\underline{M}, \bar{M} \in \mathbb{R}_{>0}$  are known constants.

*Property 2:*  $\dot{M} \leq c_M |\dot{q}|$ , where  $c_M \in \mathbb{R}_{>0}$  is a known constant.

*Property 3:*  $|V(q(t), \dot{q}(t))| \leq c_V |\dot{q}(t)|$ , where  $c_V \in \mathbb{R}_{>0}$  is a known constant.

*Property 4:*  $0 < b_{\text{cycle}} < \bar{b}$ , where  $\bar{b} \in \mathbb{R}_{>0}$  is a known constant.

*Property 5:*  $|G(q(t))| \leq c_G$ , where  $c_G \in \mathbb{R}_{>0}$  is a known constant.

*Property 6:*  $|P(q(t), \dot{q}(t))| \leq c_{P_1} + c_{P_2} |\dot{q}(t)|$ , where  $c_{P_1}, c_{P_2} \in \mathbb{R}_{>0}$  are known constants [24].

*Property 7:*  $0 < c_b \leq B_\sigma \leq c_B$ , where  $c_b, c_B \in \mathbb{R}_{>0}$  are known constants.

*Property 8:*  $\dot{M}(q(t), \dot{q}(t)) - 2V(q(t), \dot{q}(t)) = 0$  by skew symmetry.

### III. MAIN RESULTS

In this section, the control input error  $u_{\text{ce}}(t)$  is defined such that the learning control input  $u_l(t)$  converges to the desired control input  $u_d(t)$ , i.e.,  $u_l \rightarrow u_d$ . The analysis to achieve the cadence tracking can be examined through the following two theorems. Theorem 1 shows that the closed-loop switched system is the output strictly passive (OSP). Theorem 2 shows that the learning controller ensures the  $\mathcal{L}_2$  convergence of the cadence tracking error.

#### A. Control Development

The control objective is to track a desired crank trajectory. The tracking error signals  $e_1, e_2 : \mathbb{R}_{\geq 0} \rightarrow \mathbb{R}$  are defined as

$$e_1(t) = q(t) - q_d(t) \quad (9)$$

$$e_2(t) = \dot{e}_1(t) + \alpha e_1(t) \quad (10)$$

where  $q_d : \mathbb{R}_{\geq 0} \rightarrow \mathbb{R}$  is the desired crank position such that its derivative exists and  $|\dot{q}_d| \leq c_{d_1}$ ,  $|\ddot{q}_d| \leq c_{d_2}$ , where  $c_{d_1}, c_{d_2} \in \mathbb{R}_{>0}$  are known constants, and  $\alpha \in \mathbb{R}_{>0}$  is a positive constant. Since the objective is to follow the desired crank trajectory,  $e_2(t)$  in (10) is considered as the output of the system. We propose the control input error as

$$u_{\text{ce}}(t) = u_l(t) - u_d(t) \quad (11)$$

where  $u_l : \mathbb{R}_{\geq 0} \rightarrow \mathbb{R}$  is the learning control input and will be designed later based on ITC techniques, and  $u_d : \mathbb{R}_{\geq 0} \rightarrow \mathbb{R}$  is the bounded ideal input. Based on the open-loop dynamics in (7) and the subsequent stability analysis, the controller is designed as

$$u(t) = -k_1 e_2 - k_2 |e_2| - k_3 |e_1| |e_2| - k_4 \text{sgn}(e_2) + u_l \quad (12)$$

where  $k_1, k_2, k_3, k_4 \in \mathbb{R}_{>0}$  are positive constants and  $\text{sgn} : \mathbb{R} \rightarrow [-1, 1]$  is the signum function. Substituting (12) into (7) yields

$$\begin{aligned} M(q(t))\ddot{q}(t) + V(q(t), \dot{q}(t))\dot{q}(t) + b_{\text{cycle}}\dot{q}(t) \\ + G(q(t)) + P(q(t), \dot{q}(t)) + d_r(t) \\ = B_\sigma(q(t), \dot{q}(t))(-k_1 e_2 - k_2 |e_2| \\ - k_3 |e_1| |e_2| - k_4 \text{sgn}(e_2)) + B_\sigma(q(t), \dot{q}(t))u_l(t). \end{aligned} \quad (13)$$

After some algebraic manipulation, the closed-loop dynamics can be expressed as

$$\begin{aligned} M(q)\ddot{e}_1 + V(q, \dot{q})\dot{e}_1 + b_{\text{cycle}}\dot{e}_1 + \chi \\ = B_\sigma(q, \dot{q})(-k_1 e_2 - k_2 |e_2| - k_3 |e_1| |e_2| \\ - k_4 \text{sgn}(e_2)) + B_{\sigma_e}(q, \dot{q})u_{\text{ce}} \end{aligned} \quad (14)$$

where

$$\begin{aligned} \chi = (M(q) - M(q_d))\ddot{q}_d + (V(q, \dot{q}) - V(q_d, \dot{q}_d))\dot{q}_d \\ + (G(q) - G(q_d)) + P(q, \dot{q}) + d_r(t) \end{aligned} \quad (15)$$

and

$$B_{\sigma_e}(q(t), \dot{q}(t)) = \min\{B_\sigma(q(t), \dot{q}(t)), B_\sigma(q_d(t), \dot{q}_d(t))\} \quad (16)$$

$0 < c_{b_e} \leq B_{\sigma_e} \leq c_{B_e}$ , where  $c_{b_e}, c_{B_e} \in \mathbb{R}_{>0}$  are known constants.

### B. Passive Motorized FES Cycle and Rider Dynamics

To facilitate the subsequent analysis and using Properties 1–6, positive constants  $c_1, c_2, c_3, c_4, c_5 \in \mathbb{R}_{>0}$  are defined as

$$\begin{cases} c_1 = \alpha \bar{M} c_{d_2} + \alpha c_G + \alpha c_V c_{d_1}^2 \\ c_2 = 1 + \alpha \bar{b} + \bar{M} c_{d_2} + c_G + c_V c_{d_1}^2 + \alpha c_V c_{d_1} \\ \quad + \frac{1}{2} \alpha c_M c_{d_1} + \alpha c_{P_2} \\ c_3 = \alpha \bar{M} + \bar{b} + c_V c_{d_1} + c_{P_2} \\ c_4 = \frac{1}{2} \alpha c_M \\ c_5 = c_d + c_{P_1} + c_{P_2} c_{d_1}. \end{cases} \quad (17)$$

*Theorem 1:* Consider the closed-loop system in (14). If the positive gains  $k_1, k_2, k_3, k_4$  and the constant  $\alpha$  are selected such that

$$\bar{M} < \frac{1}{\alpha^2} \quad (18)$$

$$k_1 > 0 \quad (19)$$

$$c_b^{-1} c_3 < k_2 < \frac{c_1 c_3 - \frac{1}{4} c_2^2}{\alpha^2 c_b c_3 + c_1 c_b - \alpha c_b c_2} \quad (20)$$

$$k_3 > c_b^{-1} c_4 \quad (21)$$

$$k_4 > c_b^{-1} c_5 \quad (22)$$

then the closed loop system (14) from the input  $u_{ce}$  to the output  $e_2$  is OSP.

*Proof:* Consider a storage function  $V_s(t)$  as

$$V_s = \frac{1}{2} M \dot{e}_1^2 + \frac{1}{2} e_1^2 + \alpha M e_1 \dot{e}_1 \quad (23)$$

and can be expressed as

$$V_s = \frac{1}{2} M e_2^2 + \frac{1}{2} e_1^2 - \frac{1}{2} \alpha^2 M e_1^2 \quad (24)$$

which is positive, provided (18) is satisfied.

Let  $z(t) \triangleq [e_1(t) \dot{e}_1(t)]^T$  and  $z(t)$  be a Filippov solution to the differential inclusion  $\dot{z}(t) \in K[h](z(t))$ , where  $K[\cdot]$  is defined in [26] and  $h$  is defined by (10) and (14) as [27]

$$h \triangleq \begin{bmatrix} h_1 \\ h_2 \end{bmatrix} = \begin{bmatrix} \ddot{e}_1 \\ \dot{e}_1 \end{bmatrix}. \quad (25)$$

Since (14) contains the sigmoid function and the discontinuous control effectiveness  $B_\sigma$  and  $B_{\sigma_e}$ , the time derivative of the storage function exists almost everywhere (a.e.), i.e., for almost all  $t$ . According to [28, Lemma 1], the time derivative of the storage function can be obtained such that  $\dot{V}_s \stackrel{a.e.}{\in} \dot{V}$ , where  $\dot{V}$  is the generalized time derivative of (23) along the Filippov trajectories of  $\dot{z} \in h(z)$  and is defined as

$$\dot{V} \triangleq \bigcap_{\zeta \in \partial V} \zeta^T K \begin{bmatrix} \ddot{e}_1 \\ \dot{e}_1 \\ 1 \end{bmatrix}. \quad (26)$$

The storage function is continuously differentiable in  $z$ ,  $\partial V = \{\nabla V\}$ , thus

$$\begin{aligned} \dot{V} \stackrel{a.e.}{=} & \dot{e}_1 e_1 + \alpha M \dot{e}_1^2 + \frac{1}{2} \alpha \dot{M} \dot{e}_1 e_1 - b_{\text{cycle}} \dot{e}_1^2 - \alpha b_{\text{cycle}} \dot{e}_1 e_1 \\ & - \chi(\dot{e}_1 + \alpha e_1) + B_{\sigma_e}(q, \dot{q}) u_{ce} e_2 - k_1 B_\sigma(q, \dot{q}) e_2^2 \\ & - k_2 B_\sigma(q, \dot{q}) |e_2| e_2 - k_3 B_\sigma(q, \dot{q}) |e_1| |e_2| e_2 \\ & - k_4 B_\sigma(q, \dot{q}) |e_2|. \end{aligned} \quad (27)$$

After using Properties 1–8 and algebraic manipulation, (27) can be upper bounded by using the mean value theorem as

$$\begin{aligned} \dot{V} \leq & - \left( \frac{1}{c_{b_e}} \right) \Gamma_1 |e_2| - \left( \frac{1}{c_{b_e}} \right) \begin{bmatrix} |e_1| \\ |\dot{e}_1| \end{bmatrix}^T \Gamma_2 \begin{bmatrix} |e_1| \\ |\dot{e}_1| \end{bmatrix} \\ & - \left( \frac{1}{c_{b_e}} \right) \begin{bmatrix} |e_1|^2 \\ |\dot{e}_1|^2 \end{bmatrix}^T \Gamma_3 \begin{bmatrix} |\dot{e}_1| \\ |e_1| \end{bmatrix} - \left( \frac{c_b}{c_{b_e}} \right) k_1 e_2^2 + e_2 u_{ce} \end{aligned} \quad (28)$$

where

$$\Gamma_1 = k_4 c_b - c_5, \quad (29)$$

$$\Gamma_2 = \begin{bmatrix} \alpha^2 c_b k_2 - c_1 & \frac{1}{2} (2\alpha c_b k_2 - c_2) \\ \frac{1}{2} (2\alpha c_b k_2 - c_2) & c_b k_2 - c_3 \end{bmatrix} \quad (30)$$

$$\Gamma_3 = \begin{bmatrix} 2\alpha c_b k_3 & \alpha^2 c_b k_3 \\ 0 & c_b k_3 - c_4 \end{bmatrix}. \quad (31)$$

Note that  $\Gamma_1, \Gamma_2$ , and  $\Gamma_3$  are positive definite matrices provided (20), (21), and (22) are satisfied.

Integrating both sides of (28) and rearranging the terms yields

$$\begin{aligned} & \int_0^t e_2 u_{ce} d\tau \\ & \geq \tilde{V}(e_1(t), \dot{e}_1(t)) - \tilde{V}(e_1(0), \dot{e}_1(0)) \\ & \quad + \left( \frac{1}{c_{b_e}} \right) \int_0^t \Gamma_1 |e_2| d\tau + \left( \frac{1}{c_{b_e}} \right) \int_0^t \begin{bmatrix} |e_1| \\ |\dot{e}_1| \end{bmatrix}^T \Gamma_2 \begin{bmatrix} |e_1| \\ |\dot{e}_1| \end{bmatrix} d\tau \\ & \quad + \left( \frac{1}{c_{b_e}} \right) \int_0^t \begin{bmatrix} |e_1|^2 \\ |\dot{e}_1|^2 \end{bmatrix}^T \Gamma_3 \begin{bmatrix} |\dot{e}_1| \\ |e_1| \end{bmatrix} d\tau + k_1 \left( \frac{c_b}{c_{b_e}} \right) \int_0^t e_2 e_2 d\tau. \end{aligned} \quad (32)$$

The inequality in (32) can be further lower bounded as

$$\int_0^t e_2 u_{ce} d\tau \geq -\tilde{V}(e_1(0), \dot{e}_1(0)) + k_1 \left( \frac{c_b}{c_{b_e}} \right) \int_0^t e_2 e_2 d\tau. \quad (33)$$

The passivity inequality is satisfied through (33), and the closed-loop system from the input  $u_{ce}$  to the output  $e_2$  is OSP [16]. Note that  $\tilde{V}(e_1(0), \dot{e}_1(0))$  is the initial condition of the generalized storage function  $\tilde{V}(e_1(t), \dot{e}_1(t))$ . ■

### C. Iterative Learning Control for Automatic Cycle and Rider Dynamics

Theorem 1 established the OSP property for the closed-loop system in Section III-B. A learning update law  $u_l$  is designed in this section inspired by the ILC framework of [19]. The cadence tracking task is modeled as a repetitive process that ends in finite time, i.e., the duration of the  $k$ th iteration is finite from 0 to  $T$ , where  $T$  denotes the time when a single iteration ends (another notation would be to denote time as ranging from  $t^k$  to  $t^{k+1}$  for the  $k$ th iteration). Different from the initial resetting condition typically enforced in ILC (i.e., state resetting at the beginning of a new iteration), the initial state of the system at the beginning of each iteration follows from the previous iteration (i.e., the position and velocity tracking errors are continuously updated, which implies that the state is not discretely reset, thus preventing discontinuities

in the tracking task). Given the repetitive nature of the cycling objective, the iterative learning law is developed and examined for each  $k$ th iteration as

$$u_l^{k+1}(t) = u_l^k(t) - k_l e_2^k(t) \quad (34)$$

where  $k_l \in \mathbb{R}_{>0}$  is a positive constant gain.

*Theorem 2:* The convergence of  $|e_2^k(t)|$  to zero is guaranteed in the  $\mathcal{L}_2$  norm sense provided the gain conditions in (18)–(22) are satisfied and

$$0 < k_l < 2k_1 \left( \frac{c_b}{c_{b_e}} \right). \quad (35)$$

*Proof:* The learning control input error in (11) can be rewritten as

$$u_{ce}^{k+1} = u_l^{k+1} - u_d^{k+1} \quad (36)$$

$$u_{ce}^k = u_l^k - u_d^k. \quad (37)$$

Subtracting (37) from (36) and using (34) yields

$$u_{ce}^{k+1} = u_{ce}^k - k_l e_2^k. \quad (38)$$

Squaring (38) and multiplying by  $k_l^{-1}$  yields

$$k_l^{-1} (u_{ce}^{k+1})^2 = k_l^{-1} (u_{ce}^k)^2 - 2u_{ce}^k e_2^k + k_l (e_2^k)^2. \quad (39)$$

Integrating (39) from 0 to  $T$  results in

$$\begin{aligned} k_l^{-1} \int_0^T (u_{ce}^{k+1})^2 d\tau &= k_l^{-1} \int_0^T (u_{ce}^k)^2 d\tau \\ &\quad - 2 \int_0^T u_{ce}^k e_2^k d\tau + k_l \int_0^T (e_2^k)^2 d\tau \end{aligned} \quad (40)$$

which can be simplified as

$$k_l^{-1} \|u_{ce}^{k+1}\|_2 = k_l^{-1} \|u_{ce}^k\|_2 + k_l \|e_2^k\|_2 - 2 \int_0^T u_{ce}^k e_2^k d\tau. \quad (41)$$

After substituting the passivity inequality from (32), the following inequality can be developed

$$\begin{aligned} &k_l^{-1} (\|u_{ce}^{k+1}\|_2 - \|u_{ce}^k\|_2) \\ &\leq -2(\tilde{V}^k(e_1(T), \dot{e}_1(T)) \\ &\quad - \tilde{V}^k(e_1(0), \dot{e}_1(0))) - \left( \frac{2}{c_{b_e}} \right) \int_0^T \Gamma_1 |\dot{e}_1^k + \alpha e_1^k| d\tau \\ &\quad - \left( \frac{2}{c_{b_e}} \right) \int_0^T \left[ \begin{array}{c} |e_1^k| \\ |\dot{e}_1^k| \end{array} \right]^T \Gamma_2 \left[ \begin{array}{c} |e_1^k| \\ |\dot{e}_1^k| \end{array} \right] d\tau \\ &\quad - \left( \frac{2}{c_{b_e}} \right) \int_0^T \left[ \begin{array}{c} |e_1^k|^2 \\ |\dot{e}_1^k|^2 \end{array} \right]^T \Gamma_3 \left[ \begin{array}{c} |e_1^k| \\ |\dot{e}_1^k| \end{array} \right] d\tau \\ &\quad - \left( 2k_1 \left( \frac{c_b}{c_{b_e}} \right) - k_l \right) \|e_2^k\|_2. \end{aligned} \quad (42)$$

The inequality (42) implies that  $\|u_{ce}^k\|_2 + 2\tilde{V}^k(e_1(0), \dot{e}_1(0))$  is monotonically decreasing and bounded below as long as (35) holds. This confirms that  $e_2^k \rightarrow 0$  in the  $\mathcal{L}_2$  norm sense. Furthermore, from (9) and (10),  $e_1 \rightarrow 0$  when  $e_2 \rightarrow 0$ , which means that the crank trajectory will follow the desired path as  $k \rightarrow \infty$ . ■

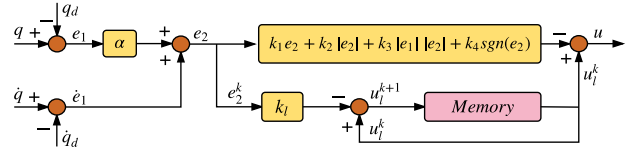


Fig. 2. Block diagram of iterative learning controller.

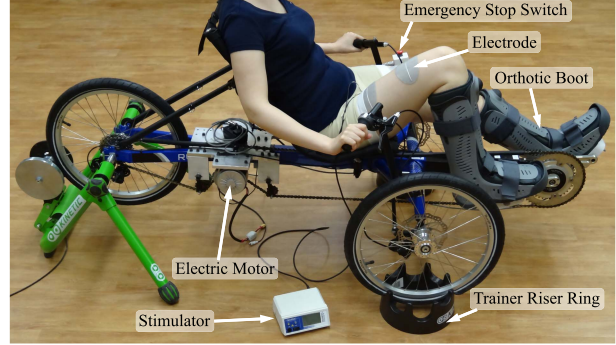


Fig. 3. Motorized FES-cycling test bed used for the experiment.

*Remark 1:* Theorem 2 states that the output of the closed-loop system, i.e., (14), which satisfies the OSP property based on Theorem 1, converges to zero in the  $\mathcal{L}_2$  norm sense as  $k \rightarrow \infty$ . Since the system is zero-state observable, the asymptotic stability of the system can also be concluded [17, Lemma 6.7]. The block diagram of the iterative learning controller is shown in Fig. 2.

## IV. EXPERIMENTS

FES-cycling experiments were performed to demonstrate the tracking performance of the designed controller with iterative learning in (5), (6), (12), and (34). Seven able-bodied subjects (two female, five male) participated in the experiments. Each subject gave written informed consent approved by the University of Florida Institutional Review Board. All participants were asked to relax and make no volitional effort to assist the cycling and were not informed of the desired trajectory, and could not see the desired or actual trajectory. In these experiments, only the quadriceps femoris muscle groups were stimulated. For safety considerations, the subject could stop the experiment at any time by using an emergency stop switch.

### A. Instrumentation

The motorized FES-cycling test bed used in the study (Fig. 3), was instrumented like in [24]. A current-controlled stimulator (RehaStim, Hasomed GmbH) operating in Science Mode delivered biphasic, symmetric, and rectangular pulses to the quadriceps muscle groups. The stimulation pulsewidth for each muscle group was determined by  $u_m$  and commanded to the stimulator by the control software. Self-adhesive PALS electrodes (3 in  $\times$  5 in)<sup>1</sup> were placed on each muscle group.

<sup>1</sup>Surface electrodes for the study were provided compliments of Axelgaard Manufacturing Co., Ltd.

The stimulation amplitudes and frequency for the quadriceps muscle groups were fixed at 90 mA and 60 Hz, respectively. The controller in (12) was implemented on a personal computer (Windows 8 OS) running a real-time target (QUARC 2.5, Quanser) via MATLAB/Simulink 2015b (MathWorks Inc) with a sample rate of 500 Hz.

### B. Experimental Setup

Electrodes were placed over the subjects' quadriceps femoris muscle groups according to Axelgaard's electrode placement manual.<sup>2</sup> Seat position adjustments were performed at the beginning of each experiment to ensure a proper interaction between the subject and the tricycle. The distance from the cycle crank to the subject's right greater trochanter was measured according to [24], preventing full knee extension. The torque transfer ratio for subjects' muscle groups was calculated based on the geometric measurements of each individual. Each experiment lasted between 180 and 300 s, depending on the subject. Two primary factors determined if an experiment was terminated before 300 s, mainly if the subject's sensitivity to stimulation produced an uncomfortable sensation or if the cadence tracking error increasing above a range of  $\pm 5$  rpm at steady state. The desired cadence was designed to smoothly reach 50 rpm, remaining at this value for the duration of the experiment. The desired crank velocity  $\dot{q}_d$  was defined in radians per second [24] as

$$\dot{q}_d \triangleq \frac{5\pi}{3}(1 - e^{-\frac{2}{5}t}). \quad (43)$$

To avoid exerting large muscle forces at the beginning of the experiment, the motor was initially activated and the muscle stimulation intensities were progressively incorporated. The motor was active for the first 16 s of the experiment until the cadence reached 50 rpm, then the muscle intensities were gradually increased during a transition period of 10 s until the desired steady state stimulation pattern was achieved. After this transition, the learning update law in (34) is activated to track the constant 50 rpm cadence trajectory. The control gains and the learning control gain in (5), (12), and (34) and the constant  $\alpha$  in (10) were tuned prior to each experiment to achieve a proper tracking performance and they were selected as  $\alpha = 2$ ,  $k_m = 0.5$ ,  $k_e = 1$ ,  $k_l \in [1.5, 3.5]$ ,  $k_{m1} \in [65, 111]$ ,  $k_{m2} = 0.25$ ,  $k_{m3} \in [5, 7.5]$ ,  $k_{m4} \in [0.5, 1]$ ,  $k_{e1} = 13.5$ ,  $k_{e2} = 0.09$ ,  $k_{e3} = 4.5$ ,  $k_{e4} = 0.09$ , where subscript  $m$  refers to the muscle controller gains and subscript  $e$  refers to the motor controller gains.

### C. Results

The tracking performance for Subject 1, quantified by the cadence tracking error  $\dot{e}_1$  and the root mean square (RMS), is depicted in Fig. 4. Fig. 5 shows the stimulation intensity input to each muscle group  $u_m$  and the electric motor current input  $u_e$ . In Fig. 6, the distribution of the control input between FES and the motor across one crank cycle for Subject 1 is represented. Fig. 7 illustrates a closer look at the stimulation intensity input to each muscle group  $u_m$ , the electric motor

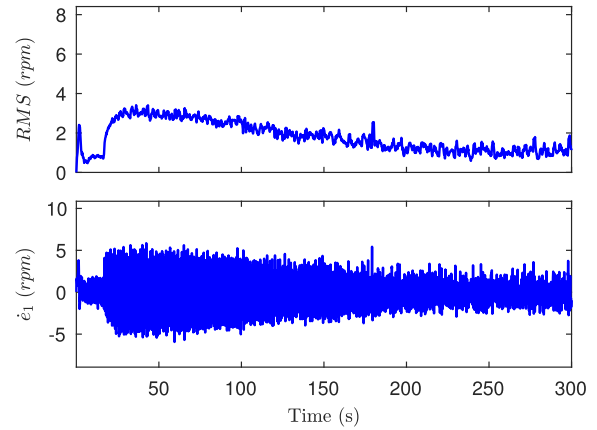


Fig. 4. Tracking performance for Subject 1 characterized by the cadence tracking error  $\dot{e}_1$  and its RMS over  $t \in [0, 300]$ .

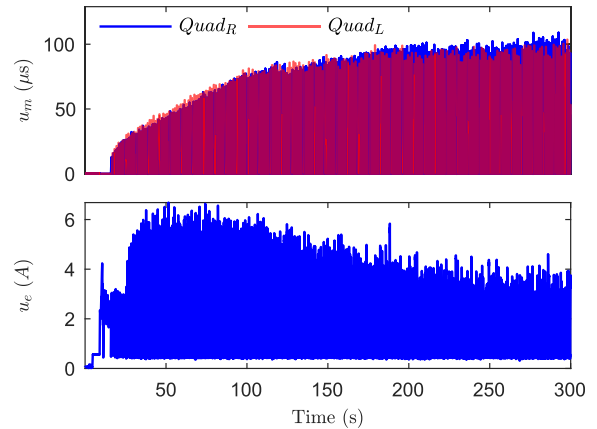


Fig. 5. FES control input to quadriceps femoris muscle groups  $u_m$  and the electric motor current input  $u_e$  for Subject 1 over  $t \in [0, 300]$ .

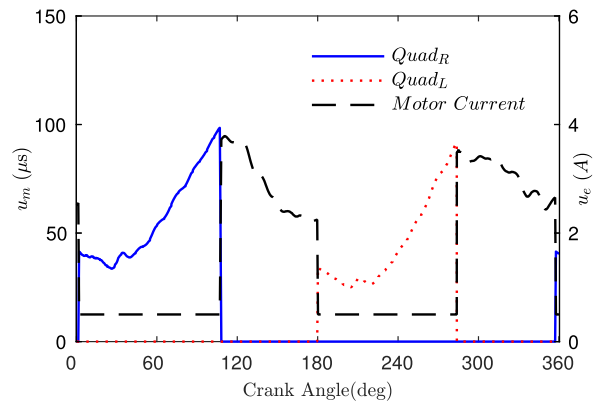


Fig. 6. Switched control input among FES quadriceps femoris muscle groups and electric motor over a single crank cycle for Subject 1.

current input  $u_e$ , the learning control input  $u_l$ , and the cadence tracking error  $\dot{e}_1$  over four revolutions for Subject 1. Table I summarizes the transitory and steady state of the RMS, the cadence tracking error  $\dot{e}_1$ , and the percentage of error for Subjects 1–7.

<sup>2</sup><http://www.palsclinicalsupport.com/videoElements/videoPage.php>

TABLE I  
SUMMARY OF AUTOMATIC CYCLE-RIDER SYSTEM PERFORMANCE FOR SEVEN SUBJECTS. THE TRANSITORY AND STEADY STATE OF THE RMS, THE CADENCE TRACKING ERROR  $\dot{e}_1$ , AND THE PERCENTAGE OF ERROR

	RMS		$\dot{e}_1$		% Error	
	Transitory	Steady State	Transitory	Steady State	Transitory	Steady State
Subject 1	2.20±0.64	1.83±0.73	0.07±2.98	-0.01±1.92	0.42±4.79	-0.02±3.93
Subject 2	2.32±0.60	2.72±0.29	0.04±2.93	0.00±2.73	0.45±4.97	-0.00±5.48
Subject 3	1.58±0.46	1.86±0.53	0.04±2.55	-0.01±1.91	0.29±3.40	-0.03±3.88
Subject 4	2.11±0.65	1.97±0.40	-0.03±2.55	-0.00±1.99	0.16±4.59	-0.01±4.03
Subject 5	2.09±0.61	2.82±0.20	0.02±2.82	-0.01±2.83	0.26±4.61	-0.03±5.66
Subject 6	2.22±0.69	2.88±0.28	-0.10±2.98	-0.00±2.89	0.54±4.88	-0.02±5.79
Subject 7	2.49±0.61	3.00±0.17	0.02±2.96	-0.00±3.00	0.23±5.29	-0.00±6.01
Mean	2.15	2.44	0.01	-0.00	0.34	-0.01
STD	0.28	0.52	0.02	0.00	0.13	0.01

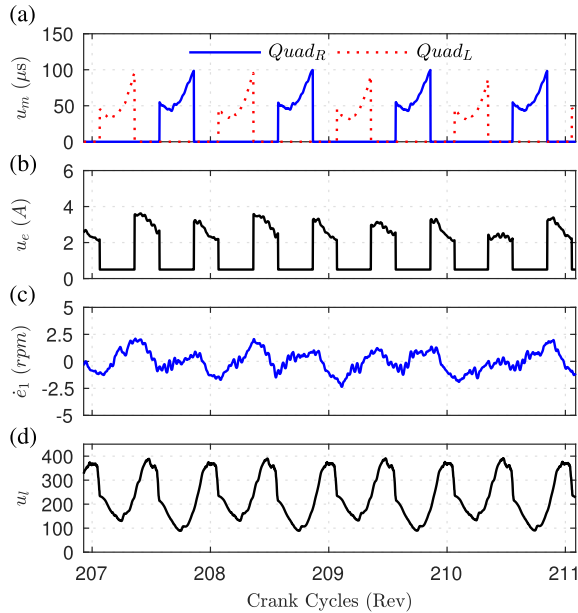


Fig. 7. Zoom-in representation of the FES control input  $u_m$ , the electric motor control input  $u_e$ , the learning control input  $u_l$ , and the cadence tracking error  $\dot{e}_1$  over four revolutions for Subject 1.

#### D. Discussions

The control strategy was developed based on the passivity concept, and the switched input was properly distributed between the FES control input  $u_m$  and the electric motor  $u_e$ . The results show that the learning controller was able to successfully regulate the cadence tracking error  $\dot{e}_1$  close to zero. Note that the exact zero convergence could not be achieved due to unknown disturbances such as the electromechanical delay between the muscle activation and the force production [29] and the muscle fatigue. The RMS of the cadence tracking error in Fig. 4 clearly illustrates the transitory and steady state behavior of the cadence tracking error  $\dot{e}_1$ , showing the convergence of the cadence tracking error for Subject 1. As evident from Fig. 7(c),  $\dot{e}_1$  has a steady-state error of  $\pm 2.47$  rpm. In addition, Fig. 7(d) shows the contribution of the learning controller  $u_l$  over the same revolutions.

#### V. CONCLUSION

The passivity property of an automatic stationary cycle where cycling is either produced by motorized assistance

or induced through muscle stimulation was studied. Due to the uncertain nonlinear dynamics of the switched closed-loop system, and the repetitive nature of the cycling task, ILC was used to achieve the desired output trajectory. The developed method ensured the  $\mathcal{L}_2$  norm of the output error trajectory converges to zero. The OSP property of the system was proven, and the ILC scheme based on the Arimoto learning control update law was developed. Results obtained from the experiments on a recumbent stationary bicycle for seven able-bodied participants, where the average cadence tracking error was  $0.00 \pm 2.47$  rpm ( $0.01 \pm 4.97\%$  error) for 50 rpm at steady state. Future work will investigate the implementation of this learning control technique in participants with neurological conditions to elucidate the long-term benefits of this rehabilitative intervention. Moreover, a similar approach could be investigated for the control of upper limbs such as hand cycling. Open questions also remain regarding the optimal interplay between motor assistance and induced or voluntary effects by individuals, stimulation thresholds related to participant sensitivity, and effects of specific neurological conditions.

#### REFERENCES

- [1] A. R. Kralj and T. Bajd, *Functional Electrical Stimulation: Standing and Walking After Spinal Cord Injury*. Boca Raton, FL, USA: CRC Press, 1989.
- [2] G. M. Davis, N. A. Hamzaid, and C. Fornusek, "Cardiorespiratory, metabolic, and biomechanical responses during functional electrical stimulation leg exercise: Health and fitness benefits," *Artif. Organs*, vol. 32, no. 8, pp. 625–629, 2008.
- [3] A. H. Vette, K. Masani, and M. R. Popovic, "Implementation of a physiologically identified PD feedback controller for regulating the active ankle torque during quiet stance," *IEEE Trans. Neural Syst. Rehabil. Eng.*, vol. 15, no. 2, pp. 235–243, Jun. 2007.
- [4] M. Ferrarin, E. D'Acquisto, A. Mingrino, and A. Pedotti, "An experimental PID controller for knee movement restoration with closed loop FES system," in *Proc. 18th Annu. Int. Conf. IEEE Eng. Med. Biol. Soc.*, vol. 1, Nov. 1996, pp. 453–454.
- [5] E. Idsø, T. Johansen, and K. Hunt, "Finding the metabolically optimal stimulation pattern for FES-cycling," *Power*, vol. 10, no. 12, p. 14, 2004.
- [6] N. Kirsch, N. Alibeji, B. E. Dicianno, and N. Sharma, "Switching control of functional electrical stimulation and motor assist for muscle fatigue compensation," in *Proc. IEEE Amer. Control Conf. (ACC)*, Jul. 2016, pp. 4865–4870.
- [7] K. J. Hunt *et al.*, "Control strategies for integration of electric motor assist and functional electrical stimulation in paraplegic cycling: Utility for exercise testing and mobile cycling," *IEEE Trans. Neural Syst. Rehabil. Eng.*, vol. 12, no. 1, pp. 89–101, Mar. 2004.
- [8] S. Arimoto, S. Kawamura, and F. Miyazaki, "Bettering operation of dynamic systems by learning: A new control theory for servomechanism or mechatronics systems," in *Proc. 23rd IEEE Conf. Decis. Control*, vol. 23, Dec. 1984, pp. 1064–1069.

- [9] H. Dou, K. K. Tan, T. H. Lee, and Z. Zhou, "Iterative learning feedback control of human limbs via functional electrical stimulation," *Control Eng. Pract.*, vol. 7, no. 3, pp. 315–325, 1999.
- [10] T. Seel, C. Werner, J. Raisch, and T. Schauer, "Iterative learning control of a drop foot neuroprosthesis—Generating physiological foot motion in paretic gait by automatic feedback control," *Control Eng. Pract.*, vol. 48, pp. 87–97, Mar. 2016.
- [11] V. H. Duenas, C. A. Cousin, A. Parikh, and W. E. Dixon, "Functional electrical stimulation induced cycling using repetitive learning control," in *Proc. IEEE 55th Conf. Decis. Control (CDC)*, Dec. 2016, pp. 2190–2195.
- [12] C. T. Freeman, "Upper limb electrical stimulation using input-output linearization and iterative learning control," *IEEE Trans. Control Syst. Technol.*, vol. 23, no. 4, pp. 1546–1554, Jul. 2015.
- [13] M. Sun, S. S. Ge, and I. M. Y. Mareels, "Adaptive repetitive learning control of robotic manipulators without the requirement for initial repositioning," *IEEE Trans. Robot.*, vol. 22, no. 3, pp. 563–568, Jun. 2006.
- [14] T. Lin, D. H. Owens, and J. Hätönen, "Newton method based iterative learning control for discrete non-linear systems," *Int. J. Control*, vol. 79, no. 10, pp. 1263–1276, 2006.
- [15] W. Messner, R. Horowitz, W.-W. Kao, and M. Boals, "A new adaptive learning rule," *IEEE Trans. Autom. Control*, vol. 36, no. 2, pp. 188–197, Feb. 1991.
- [16] A. Van der Schaft, *L<sub>2</sub>—Gain and Passivity Techniques in Nonlinear Control*. London, U.K.: Springer, 2012.
- [17] H. K. Khalil and J. Grizzle, *Nonlinear Systems*, vol. 3. Upper Saddle River, NJ, USA: Prentice-Hall, 1996.
- [18] B. Bernard, L. Ioan-Dore, and L. L. Rogelio, "Adaptive motion control of robot manipulators: A unified approach based on passivity," *Int. J. Robust Nonlinear Control*, vol. 1, no. 3, pp. 187–202, 1991.
- [19] S. Arimoto, H.-Y. Han, P. T. A. Nguyen, and S. Kawamura, "Iterative learning of impedance control from the viewpoint of passivity," *Int. J. Robust Nonlinear Control*, vol. 10, no. 8, pp. 597–609, 2000.
- [20] H. Kawai, T. Murao, R. Sato, and M. Fujita, "Passivity-based control for 2DOF robot manipulators with antagonistic bi-articular muscles," in *Proc. IEEE Int. Conf. Control Appl. (CCA)*, Sep. 2011, pp. 1451–1456.
- [21] Y. Ichijo, T. Murao, H. Kawai, and M. Fujita, "Passivity-based iterative learning control for 2DOF robot manipulators with antagonistic bi-articular muscles," in *Proc. IEEE Conf. Control Appl. (CCA)*, Oct. 2014, pp. 234–239.
- [22] E. S. Idsø "Development of a mathematical model of a rider-tricycle system," Dept. Eng. Cybern., Norwegian Univ. Sci. Technol., Trondheim, Norway, Tech. Rep., 2002. [Online]. Available: <http://citeseerx.ist.psu.edu/viewdoc/download?doi=10.1.1.152.9005&rep=rep1&type=pdf>
- [23] D. Liberzon, *Switching in Systems and Control*. New York, NY, USA: Springer, 2012.
- [24] M. J. Bellman, R. J. Downey, A. Parikh, and W. E. Dixon, "Automatic control of cycling induced by functional electrical stimulation with electric motor assistance," *IEEE Trans. Autom. Sci. Eng.*, vol. 14, no. 2, pp. 1225–1234, Apr. 2017.
- [25] M. J. Bellman, T.-H. Cheng, R. J. Downey, C. J. Hass, and W. E. Dixon, "Switched control of cadence during stationary cycling induced by functional electrical stimulation," *IEEE Trans. Neural Syst. Rehabil. Eng.*, vol. 24, no. 12, pp. 1373–1383, Dec. 2016.
- [26] A. F. Filippov, *Differential Equations With Discontinuous Righthand Sides*, vol. 18. Dordrecht, The Netherlands: Springer, 2013.
- [27] B. Paden and S. Sastry, "A calculus for computing Filippov's differential inclusion with application to the variable structure control of robot manipulators," *IEEE Trans. Circuits Syst.*, vol. CAS-34, no. 1, pp. 73–82, Jan. 1987.
- [28] N. Fischer, R. Kamalapurkar, and W. E. Dixon, "LaSalle-Yoshizawa corollaries for nonsmooth systems," *IEEE Trans. Autom. Control*, vol. 58, no. 9, pp. 2333–2338, Sep. 2013.
- [29] N. Sharma, C. M. Gregory, and W. E. Dixon, "Predictor-based compensation for electromechanical delay during neuromuscular electrical stimulation," *IEEE Trans. Neural Syst. Rehabil. Eng.*, vol. 19, no. 6, pp. 601–611, Dec. 2011.